

# Dynamics of “Small Galaxies” in the Hubble Deep Field

Wesley N. Colley,<sup>1</sup> Oleg Y. Gnedin, Jeremiah P. Ostriker, James E. Rhoads<sup>2</sup>  
 Princeton University Observatory, Princeton, NJ 08544

Email: wes,ognedin,jpo,rhoads@astro.princeton.edu

## ABSTRACT

We have previously found in the Hubble Deep Field a significant angular correlation of faint, high color-redshift objects on scales below one arcsecond, or several kiloparsecs in metric size. A correlation at this scale is most likely due to physical associations. We examine the correlation and nearest neighbor statistics to conclude that 38% of these objects in the HDF have a companion within one arcsecond (or about 6 kpc), three times the number expected in a random distribution with the same number of objects; the total excess approaches 1.5 objects by separations of 10 arcseconds. We next examine three possible dynamical scenarios for these object multiplets: 1) the objects are star-forming regions within normal galaxies, whose disks have been relatively dimmed by  $K$ -correction and surface brightness dimming; 2) they are fragments merging into large galaxies; 3) they are satellites accreting onto parent normal  $L_*$  galaxies. We find that hypothesis 1 is most tenable. First, large galaxies in the process of a merger formation would have accumulated too much mass in their centers ( $5 \times 10^{12} M_\odot$  inside 2 kpc) to correspond to any abundant category of present day objects. Second, accretion by dynamical friction occurs with a predictable slope in density vs. radius that is not seen among the faint HDF objects. Since the dynamical friction time is roughly (1 Gyr), a steady-state should have been reached by redshift  $z \lesssim 5$ . In the context of these two dynamical scenarios, we consider the possible effects of a gradient in mass-to-light ratio caused by induced star-formation during infall. We note that star-forming regions within galaxies clearly present no dynamical problems, but also that large spirals would still appear as such in the HDF, which leads us to favor a scenario in which the faint compact sources in the HDF are giant starforming regions within small normal galaxies, such as Magellanic irregulars. Last we note that the “excess” number of

---

<sup>1</sup>Supported by the Fannie and John Hertz Foundation, Livermore, CA 94551-5032

<sup>2</sup>Present Address: Kitt Peak National Observatory

correlated objects near a given faint source approaches 1.5, suggesting that the previous counts of objects have overestimated the number of galaxies by a factor of 2.5, while underestimating their individual luminosities by the same factor.

*Subject headings:* cosmology: observations — galaxies: structure, evolution, dynamics

## 1. Introduction

The Hubble Deep Field (Williams et al. 1995) affords us an unprecedented view of the optical sky at small angular scales and faint flux levels. The number of sources detected in the field is a dramatic increase over previous faint source counts and has led to proposals that the number of galaxies has been seriously underestimated (Williams et al. 1996) by ground-based work. However, Colley et al. (1996b) (Paper I) have argued that many of the faintest objects show strong angular correlation on the sub-arcsecond scale. For this to be so, many of the detected sources must lie within a few kiloparsecs of each other, leading to the possibility that the excess is due to fragments of galaxies mis-identified as separate objects. We now seek to assess the dynamical nature of these objects.

In section 2, we shall motivate the importance of understanding these associated multiplets by computing the probability that an object’s nearest neighbor lies within one arcsecond ( $\sim 6$  kpc), first using the correlation function, then using nearest-neighbor statistics.

Our first dynamical hypothesis, which is favored in Paper I, is that these physically associated objects are part of normal (in the present-day sense) galaxies seen at high-redshift, under the peculiar observational effects of strong  $K$ -correction and surface-brightness dimming. These effects tend to enhance strongly the relative prominence of UV-bright compact sources, such as giant star-forming regions. O’Connell & Marcum (1996) have shown that even nearby  $L_*$  spirals observed in the ultraviolet appear very spotty and clumpy. The light is dominated by active star-forming regions, while the underlying stellar disk remains virtually invisible. We showed in Paper I that the counts are consistent with this hypothesis ( $N_{objects} \propto 1/\text{flux}$ ), but do not necessitate it.

We next consider the alternative hypothesis that these subgalaxian sources are currently undergoing merging on their way to becoming present-day  $L_*$  galaxies. This hypothesis is probably the most exciting of those we will consider, because it would suggest that we have finally seen deep enough to see normal galaxies in formation. This hypothesis has been proposed by several others (cf. Odewahn et al. 1996), since large galaxies irregularly

acquiring gas on “hot-spots” where active star-formation ensues could explain the multi-peaked appearance of sources in the HDF.

We finally discuss the possibility that the sources are  $L_*$  galaxies accreting small Irregulars on the dynamical friction timescale, much as our galaxy is currently accreting the Magellanic Clouds. Again, this hypothesis is consistent with the results from Paper I, in that nearly complete accretion events could show up as multiple peaks within a small angular (and spatial) scale.

Ultimately we find that the first hypothesis is the most likely dynamically, which indicates that the object counts have overestimated galaxy counts and underestimated individual galaxy luminosities.

## 2. Small Angle Correlation Among the Faint Sources

In Paper I, we computed the angular correlation within several subsets of objects observed in the HDF. An important subset contained only objects with high color-redshifts, i.e. objects having colors most consistent with high-redshift ( $z > 2.4$ ) populations (Steidel et al. 1996). We found this subset to contain excess correlation below 0."5 as compared with the complementary set of low color-redshift objects. We plot in figure 1, for reference, the correlation of these high color-redshift objects. We have overplotted the best-fit power law, which has the form  $w_{fit} = (\theta/\theta_\ell)^\alpha$ , where  $\alpha = -1.1 \pm 0.1$  and  $\theta_\ell = 0."93 \times 10^{\pm 0.03}$ , the correlation length.

We may now compute the expected number of objects within a correlation length of a given object in the catalog as

$$\langle N(\theta < \theta_\ell) \rangle = \int_0^{\theta_\ell} 2\pi\Sigma(1+w)\theta d\theta = \pi\Sigma\theta^2 \left[ 1 + \frac{2}{\alpha+2} \left( \frac{\theta}{\theta_\ell} \right)^\alpha \right]. \quad (1)$$

where  $\Sigma$  is the mean number surface density of catalog objects in the field. For our measured values of  $\alpha$  and  $\theta_\ell$ , we have  $\langle N \rangle = 0.38$  (as compared to 0.12 with no correlation). According to Poisson statistics,  $1 - e^{-0.38} = 32\%$  of the catalog objects would have at least one other object within the correlation length.

As a further check, we cataloged all objects in each chip which had a neighbor within one arcsecond. We found that 196 of the 695 objects classified as high color-redshift (28%) had at least one neighbor within one arcsecond. Including multiplets, we have 256 total objects within an arcsecond of another ( $\langle N \rangle = 0.37$ ), in excellent agreement with the values expected from the correlation. Also note that the directly counted number of associated objects is roughly a factor of three greater than that expected from a random distribution.

We have plotted in figure 2a the distribution of the nearest neighbors. The solid histogram is the differential distribution of nearest neighbors (separation  $\theta_{nn}$ ) among high color-redshift catalog objects in the HDF. We have plotted for reference the expected distribution for a random sample with the same number of objects in the same field (dashed curve)

$$\frac{dP}{d\theta_{nn}} = e^{-N(\theta_{nn})} \frac{dN}{d\theta_{nn}}, \quad dN(\theta_{nn}) = 2\pi\Sigma\theta_{nn}d\theta_{nn}. \quad (2)$$

where  $\Sigma$ , as before, is the number surface density of catalog objects. The peak in the distribution of catalog objects occurs between 0."5 and 1."0, while in a random sample, the distribution of nearest neighbors would be expected to peak near 1".6. (As an aside we note that this result could not have been predicted simply from the correlation function. All order, not just second order, correlations are needed to predict the nearest neighbor distribution.)

Figure 2b shows the same data in a different way. In this figure we plot the number of objects within an angular radius  $\Delta\theta$  of other objects. The solid curve is for the high color-redshift objects in the HDF, the dashed curve for a random distribution. The heavy solid curve is the excess over the random distribution. We see that the significant correlation function actually translates into the number of objects expected from the correlation, denoted by the plus-sign, and that the excess over the random sample is significant with an arcsecond, and approaches 1.5 objects at large separation.

### 3. Hypothesis 1: The sources are parts of Normal Galaxies

We shall first consider this basic question: What would normal present-day galaxies look like if redshifted to  $z > 1$ ? As discussed in Paper I, two observational effects critically change the appearance of galaxies as they are redshifted away from us. The  $K$ -correction brings rest-frame ultraviolet light into the visible bands of the HDF, and surface brightness dimming favors prominence of compact (unresolved or marginally resolved) objects. Giant H II regions are both UV bright and compact, and hence shine brightly above the underlying diffuse stellar disk. The  $K$ -correction effects have been well established by O’Connell & Marcum (1996) who have imaged nearby spirals with UIT and shown them to present a very clumpy appearance where even the bulge can be less prominent than the active star-forming regions in the disk. This effect is exacerbated by preferential surface brightness dimming of diffuse objects with increasing redshift.

An excellent nearby example of a bright star-forming region in a diffuse stellar disk is 30 Doradus in the Large Magellanic Cloud (LMC). Cheng et al. (1992) have measured the UV (2558Å) flux of the inner 3' (40 pc) at 6.0 magnitudes ( $M_{UV} = -12.7$ ). The total

30 Doradus complex, however covers  $1^\circ$  (1 kpc), so that the total absolute  $U$ -magnitude of the entire complex is approximately  $-14$ . For a distance modulus of 43.7 ( $z \sim 1$ ,  $h = 0.7$ , Peebles 1993), this gives a magnitude of approximately 29.7, within the broad peak of the  $(R+I)/2$  magnitudes of objects in the Hubble Deep Field (Paper I). “Super star clusters” (as seen in starburst galaxies) can have somewhat brighter UV flux (up to around 3 magnitudes brighter, O’Connell et al.1995). Therefore, a large spread in the magnitude around 28–29 for very actively star-forming regions in the Hubble Deep Field would be expected, and is confirmed in Paper I. At a redshift of  $z = 1.0$  the 0.5 kpc radius of 30 Doradus translates to an angular radius of 0.08 arcseconds, or 80% of one p.s.f. on the WFC2. Thus we might expect many of the small objects seen in the HDF to be marginally resolved if our hypothesis were correct.

The relative  $K$ -correction between such star-forming regions and diffuse stellar disks may be quantified with stellar population synthesis models. Charlot & Bruzual (1995) report a  $(\lambda = 2700\text{\AA}) - V$  color of order  $-1.5$  in regions which have undergone a burst of star-formation  $10^7$  years ago, vs.  $-0.1$  for a 3 Gyr-old population in an exponentially declining star-formation epoch. For an old stellar disk in the same model (age of 4 Gyr), the color is 1.0. So at a redshift  $z \sim 1.5$ , a young H II region will be enhanced over a Population I disk by about 1.5 magnitudes due to  $K$ -correction alone, while the enhancement over a Population II bulge can be as great as 2.5 magnitudes.

Furthermore, while a large fraction of the light from a large star-forming region resides in one  $0.1''$  point-spread-function of the WFC2, the diffuse light of given surface magnitude only lends one-hundredth of that light to a single pixel. So, in comparison to ground-based efforts, objects which are marginally resolved from space can see a several magnitude enhancement in surface brightness over diffuse objects. Finally, fully resolved objects (such as diffuse disks) will suffer  $(1+z)^4$  dimming in bolometric surface brightness, significant particularly for higher redshift objects.

All these factors transform the surface brightness from the normal level of 21 mag/sq. arcsec to 31 mag/pixel, significantly dimmer than the star-forming regions, and close to the detection threshold of the HDF. Also, nearly all local, late-type galaxies achieve a maximum a B-surface brightness of 21 or greater in their disks (McGaugh, 1996; Patterson & Thuan 1996). Among a significant fraction of the associated faint sources, very faint (often just detectable) material connecting them is visible (cf. Steidel et al. 1996), in agreement with the hypothesis that the objects are physically associated within some underlying background medium.

This rough quantitative sketch demonstrates that giant star-forming regions possess the necessary properties to constitute many of the faint sources in the HDF, while the underlying

disks would be sufficiently dimmed from  $K$ -correction and surface brightness dimming to push them to the edge of detectability on the HDF.

In fact, we may be more specific about the nature of the hosts for these star-forming regions. O’Connell and Marcum (1996) have produced synthetic images of  $L_*$  spirals at high-redshift with the approximate resolution of the HDF. One could summarize the results by saying that, although they look a lot more clumpy, spirals still look like spirals. In M101, for instance, the H II regions can be traced around the spiral arms quite easily in these synthetic images. Since 1) we masked out obvious large spirals in our study (see Paper I), 2) most of the objects in our high color-redshift catalog have only two or three peaks (consistent with the analysis of the correlation in the previous section), and 3) the bulk of the excess correlation occurs within 6 kpc, we see that the observational evidence suggests that the objects are most akin to Magellanic irregulars, which contain one or more very bright Giant H II regions, such as 30 Doradus, that dominate the flux seen in the HDF. Obviously this is dynamically plausible, since the LMC exists.

#### 4. Hypothesis 2: The sources are Large Galaxies in Formation

In order to model the dynamics for other theoretical hypotheses, we require a mass-model for the typical multiple source system. Assuming a constant mass-to-light ratio (reasonable for coeval active star forming regions), we directly infer the mass surface density from the surface brightness, which we have plotted in figure 3. Figure 3 plots the  $(R + I)/2$  surface magnitude in catalogued sources within bins of logarithmic angular radius about other sources. This process averages the profile of light in all sources with respect to each other and is independent of choosing a “central object,” which would be a daunting task for most of these rather irregular objects. We see that the profile divides roughly into two power-laws, a steep power-law (slope =  $-2.9 \pm 0.6$ ) inside of one arcsecond, and a much shallower one outside (slope =  $-0.5 \pm 0.2$ ). This plot alone is suggestive that the dynamics inside of one arcsecond may be different from those outside, which one would expect if the multiple sources are dynamically associated within 6 kpc, as suggested in Paper I. The slopes from figure 3 will be critical in our consideration of the dynamical consequences of our hypotheses.

The most extreme dynamical hypothesis is that the HDF objects are self-gravitating objects merging into larger systems. It has been proposed recently (Burkey et al. 1994) that many faint pairs of objects seen by *Hubble Space Telescope* are undergoing mergers. The current status of the extreme merger scenario is outlined in Carlberg (1992).

To explore this hypothesis, we consider typical faint HDF sources with visual magnitude of 28.8, or  $M = -14.9$  with the adopted distance modulus for redshift  $z \gtrsim 1$ . The  $K$ -correction will shift the observed light into the  $B$  and  $U$  passbands where  $M_\odot \approx 5.5$ . Thus the UV luminosity of the median object is  $L_{med} = 1.4 \times 10^8 L_\odot$ . If these objects are really infalling dwarf galaxies, their mass-to-light ratio,  $\Upsilon$ , should be characteristic of a stellar population 3–4 Gyr old. The population synthesis models of Worthey (1994) yield  $\Upsilon_B = 2.2$  for  $t = 3$  Gyr, bringing the mass of the objects to  $3.2 \times 10^8 M_\odot$ . We will adopt this conservative estimate of  $\Upsilon$ —should dark matter contribute significantly to the mass, the corresponding increase in  $\Upsilon$  would strengthen our conclusions.

The surface brightness profile of the multiple-peak HDF objects inside a projected radius of 10 kpc can be approximated, as discussed above, by a power law  $\Sigma(R) = \Sigma_0(R/R_1)^{-\alpha}$ , with  $\alpha \approx 2.9$ ,  $\Sigma_0 = 6 \times 10^7 L_\odot \cdot \text{arcsec}^{-2}$  and  $R_1 = 1''$  (5.9 kpc with  $z \sim 1$  and  $h = 0.7$ ). Inside  $0.''4$  there are no pairs of objects, which is likely an artifact of our object detection algorithm, which requires some smoothing, and distinct separation (see Paper I). Since the slope of the light in individual (but associated) sources is fairly constant down to this radius, we will consider  $r_{in} = 0.''4$  ( $\sim 2.3$  kpc) as the radius within which accreted material must have settled (we will see that a smaller radius would only require more central density, so this estimate is also conservative).

Solving the Abel equation (Binney & Tremaine 1987) we obtain the spherically symmetric distribution of objects in three dimensions

$$\rho(r) = \frac{\alpha I(\alpha) \Upsilon \Sigma_0}{\pi R_1} \left( \frac{r}{R_1} \right)^{-\alpha-1}, \quad (3)$$

where  $I(\alpha)$  is a dimensionless integral that depends weakly on the parameter  $\alpha$ .  $I(\alpha = 2.9) \approx 0.7$ . The total mass inside the fiducial radius  $R_1$  integrates to  $M(R_1) = 1.6 \times 10^9 M_\odot$ . Although each particular system that we are observing may have a short life time, it is reasonable to assume that the observed distribution of separations persists for a long enough time, say the Hubble time at that redshift, to be in a quasi-steady state. This enables us to estimate the mass of the central system. From the continuity equation, the mass accretion rate in a spherical system at a radius  $r_{in}$  is

$$\dot{M}_{acc} = 4\pi r_{in}^2 \rho(r_{in}) v_r, \quad (4)$$

where  $\rho(r_{in})$  is the deprojected space density of the objects, and  $v_r$  is the radial infall velocity. We assume for simplicity that all objects are falling in on radial orbits with the speed determined by the central mass, i.e.  $v_r = (GM_{acc}/r_{in})^{1/2}$ . While this assumption is somewhat extreme, the order-of-magnitude of the velocity will be consistent with that used in the general merger scenario. Choosing  $r_{in} = 0.''4 \approx 2.3$  kpc, we can integrate equation (4) to

obtain the total accreted mass within  $r_{in}$

$$M_{acc}(t) = 5 \times 10^{12} \left( \frac{t}{3 \times 10^9 \text{yr}} \right)^2 M_{\odot}, \quad (5)$$

by an age of 3 billion years, the Hubble time for  $z \sim 1-2$ . This much mass inside the inner 2 kpc is obviously in contradiction with  $z = 0$  observations. Therefore this extreme merger scenario is not supported by the HDF data.

Another test for the merger hypothesis is the total merger rate over the Hubble time and the corresponding mass density of the merger remnants. We have found 695 objects in three WFC2 chips of  $72'' \times 72''$ . Since the total radial (redshift) extent of these objects is uncertain, we take it simply as the Hubble distance,  $3 \times 10^3 \text{Mpc}$ , times some factor  $\chi < 1$ . By redshift  $z \sim 1$ , we expect to see several merger remnants in each cubic megaparsec.

$$n_{merger} = 2.5 \left( \frac{h}{0.7} \right) \left( \frac{\chi}{1/3} \right)^{-1} \text{Mpc}^{-3}. \quad (6)$$

If each merger accumulates  $5 \times 10^{12} M_{\odot}$ , the total amount of mass density grossly exceeds the critical density of the Universe, and is excluded by local ( $z = 0$ ) dynamical measurements;

$$\Omega_{merger} \equiv \frac{\rho_{merger}}{\rho_{cr}} = 11 \left( \frac{h}{0.7} \right) \left( \frac{\chi}{1/3} \right)^{-1} \text{ for } \Lambda = 0. \quad (7)$$

### 5. Hypothesis 3: The sources are Accreting Satellites of a Normal Galaxy

Another initially plausible hypothesis is that the faint objects might be satellites accreting onto normal  $L_*$  galaxies due to dynamical friction within the dark matter halo. This situation is a clear analogue of the Magellanic Clouds and the Sagittarius dwarf galaxy around the Milky Way.

Assuming the isothermal distribution of the dark halo with the rotation speed of 220  $\text{km s}^{-1}$ , the infall time from  $r$  to the center due to dynamical friction is (Binney & Tremaine, 1987)

$$t_{df} = 1.0 \times 10^9 \left( \frac{r}{5.9 \text{ kpc}} \right)^2 \left( \frac{v_c}{220 \text{ km s}^{-1}} \right) \left( \frac{3.2 \times 10^8 M_{\odot}}{M} \right) \text{ yr}. \quad (8)$$

This timescale is still short enough so that all presently observed objects have enough time to sink into the center.

Dynamical friction can either deplete the initial population of objects or increase it, depending on the initial radial distribution of accreted objects. Ostriker & Turner (1979) showed that if the space number density of the objects is inversely proportional to the first power of the distance from the center,  $r$ , a steady state is achieved, because at any radius,  $r$ , as many objects sink inward as come from outside. One can write the continuity equation for the space density,  $\rho$ , in objects as

$$\frac{\partial \rho}{\partial t} = \frac{1}{r^2} \frac{\partial}{\partial r} (r^2 \rho v_r). \quad (9)$$

Substituting for  $v_r = -r/t_{df} \propto r^{-1}$ , and  $\rho \propto r^{-\alpha}$ , we have

$$\frac{\partial \rho}{\partial t} \propto (\alpha - 1) \times r^{-\alpha-2}. \quad (10)$$

The steady-state solution at  $\alpha = 1$  is apparent. If the original value of  $\alpha$  is greater than one, then a core with slope  $\alpha = 1$  develops within about the dynamical friction time at a given radius. A shelf develops at the interface between the  $\alpha = 1$  core and the  $\alpha > 1$  outer regions. If the  $\alpha$  is less than one, the interior also develops a slope of about  $\alpha = 1$  within a dynamical friction time, but the interface shows a dip between the outer shallow slope region and the inner region of greater slope. Either way, the system will eventually relax into an  $\alpha = 1$  steady-state throughout until all the mass has been accreted.

In figure 3, we have plotted the best-fit power law to the surface density distribution, which corresponds to a spatial density decreasing with a power-law slope of  $\alpha = 3.9 \pm 0.6$  inside one arcsecond. For  $\alpha = 1$ , we would expect the surface density to be decreasing only logarithmically with radius. While the data are not perfect, they obviously do not portray this very weak variation expected from dynamical friction evolution. Furthermore, inside one arcsecond, the  $\chi^2$  value for the best-fit slope is 0.98 per degree of freedom, but 15 per d.o.f. for the  $\alpha = 1$  case.

We now take the slope of the observed space distribution of the faint sources in the HDF within one arcsecond (5.9 kpc) to be  $\approx -3.9$ . Since the dynamical friction time at this radius is roughly one billion years, we expect to be observing such objects already in a steady-state with  $\alpha = 1$  by  $z \lesssim 5$  if accretion is important. Thus the slope of  $\alpha = 3.9$  inside one arcsecond is a contradiction to the expected slope.

## 6. Possible Effects of a Luminosity Gradient

In hypotheses 2 and 3 above, we have assumed that the excess in light and in number counts inside  $1''$  corresponds directly to an excess in mass. However, one could imagine that

tidal shocks and other dynamical stimuli in infalling matter might induce star-formation there, and thus reduce the mass-to-light ratio significantly with decreasing separation.

First, we consider the plausible range of  $\Upsilon$  as given by 30 Doradus at the low end, and the LMC as a whole at the high end. 30 Doradus has a mass-to-light ratio of  $\Upsilon_{min} \approx 0.01$ , while the LMC as a whole has  $\Upsilon_{max} \approx 20$ . In our merger calculation, we assumed  $\Upsilon = 2.2$ , which is conservative, since LMC is, itself, undergoing shock induced star-formation at the hands of our galaxy’s tidal field. Moreover, it would be hard to imagine that if these faint objects are really infalling merger fragments that they would be devoid of dark matter completely.

We address the possibility of a gradient in the mass-to-light ratio by considering relative slopes in number density and luminosity density as a function of radius. First, outside of  $1''$ , both the number and luminosity density go as  $r^{-1.4}$ , which implies a constant mass-to-light ratio, if the infalling objects have the same mass. If we assumed that there were no real mass excess, the number density would maintain the same power-law all the way in. To explain the observed excess in light (figure 3), one would require the mass-to-light ratio to decrease as  $\Upsilon \propto r^{2.6}$  with decreasing radius. This implies a change in mass-to-light of order 20 from 2.4 kpc to 8 kpc. This is a large change, but not impossible if significant star-formation is induced by tidal shocks.

However, under this assumption, we must check whether a varying mass-to-light is sufficient to explain the luminosity excess with no mass excess. To do so, we imagine brightening the luminosity function with decreasing radius to pull less massive objects over the flux limit. We take the number-magnitude relation observed in Paper I as  $n(> L_{limit}) \propto L_{limit}^{0.25}$  (which has a convergent integrated flux), and recall from figure 3 that  $L \propto r^{-3.9}$ , so that  $n(> L_{limit}) \propto r^{-1}$ . However, this disagrees with the observed number density, which has slope  $n \propto r^{-3}$ . The number density is significantly steeper than we would expect under this hypothesis, that induced star-formation in approaching objects explains the steep inner slope of the luminosity density. We therefore conclude that there is a real mass excess which explains the bulk of the luminosity correlation in figure 3.

Though physically motivated, and plausible, a variable  $M/L$  caused by shock-induced star-formation cannot account for the number and light excesses observed in figures 1–3, and thus our conclusions are not significantly affected by this possibility.

## 7. Conclusions

In Paper I, we discovered that the faint, high color-redshift objects detected in the Hubble Deep Field present an angular correlation which is significant at angular scales below one

arcsecond ( $\sim 6$  kpc). In this work, we have used the correlation function and nearest neighbor statistics to determine that roughly one-third of all the selected objects have a neighbor within one arcsecond, so that dynamical interactions between them must be important.

We then examined three hypotheses as to the dynamics of the faint multi-peaked sources in the Hubble Deep Field. We find that the most likely scenario is that the sources are giant star-forming regions which reside in Magellanic Irregulars in approximate steady-state.

This hypothesis is favored on several grounds. From an observational standpoint, we find that the luminosity of Giant H II regions, such as 30 Doradus and those in other local galaxies, have UV luminosities roughly consistent with the bulk of faint sources observed in the HDF, yet few if any high-redshift  $L_*$  spirals are visible in the HDF. Also, the disk of LMC would be just detectable if observed at high-redshift in the HDF, which is consistent with the faint emission seen around some of the multi-peaked sources in the HDF. Finally, the size of giant H II regions corresponds to the barely resolved apparent size of the “small galaxies.” On more theoretical grounds, dynamical arguments make quite unlikely a scenario in which the objects are infalling fragments merging into an  $L_*$  galaxy, as such a system would produce too much mass ( $\sim 5 \times 10^{12} M_\odot$ ) inside 2 kpc by  $z \sim 1$ . Furthermore,  $L_*$  spirals with orbiting satellites could not be in a steady-state with their observed number density slope. The steady-state slope of  $\rho \propto r^{-1}$  should be achieved at in roughly a dynamical time, which is 1 Gyr at one arcsecond; instead we see a slope of  $\rho \propto r^{-3.9}$ . Finally, we find that it is not possible to simultaneously explain the small angle number excess and luminosity excess with a single variable mass-to-light ratio.

We therefore suggest that very bright active starforming regions within Magellanic dwarf irregulars at  $z \gtrsim 1$  provide the bulk of the physically associated faint blue sources in the Hubble Deep Field. As a consequence, number counts can overestimate the number of galaxies by a factor of 2.5 and underestimate the individual luminosities of galaxies by the same factor.

The most straight-forward test of our favored hypothesis is to study the field with longer exposures at longer wavelengths where the underlying stellar disks should be most visible. Also, we predict a relatively small relative velocity difference between adjacent peaks at the level of  $\lesssim 50$  km/s, far below the level of  $\gtrsim 200$  km/s expected for objects which are actively merging. One recent study (Guzmán et al. 1997, submitted during the refereeing stage of this paper), has, in fact, verified that many of the faint objects in the HDF are undergoing rapid star-formation, as inferred from significant emission in lines. Moreover, recent results from gravitational lens reconstruction of high-redshift galaxies has revealed sources which have multiple intense star-forming regions within a several kiloparsec disc (Franx et al. 1997, Colley et al. 1996a).

We thank an anonymous referee for useful ideas in strengthening our conclusions. WNC is most grateful for the continued support of the Fannie and John Hertz Foundation, and partial support from NSF grant AST-9529120. OYG and JPO’s work has been partially supported by NSF grant AST-9424416, and by NASA grant NAG5-2759. JER’s work has been supported by NSF grants AST 91-17388, NASA ADP grant 5-2567, and JER’s NSF traineeship DGE-9354937. Finally, we very kindly thank the HDF team for their hard work and generosity in preparing the data for public release.

## REFERENCES

- Binney, J.J., & Tremaine, S. 1987, *Galactic Dynamics* (Princeton University Press: Princeton)
- Burkey, J. M., Keel, W. C., Windhorst, R. A., & Franklin, B. E. 1994, ApJ, 429, L13
- Charlot, S., & Bruzual, G.A., 1995, results from “galaxevpl.f” FORTRAN program
- Carlberg, R. G. 1992, ApJ, 399, L31
- Cheng, K., et al., 1992, ApJ, 395, L29
- Colley, W., Rhoads, J.E., & Ostriker, J.P., & Spergel, D.N., 1996a, ApJ, 473, L63 (Paper I)
- Colley, W., Tyson, J.A., & Turner, E.L., 1996b, ApJ, 461, L83
- Franx, M., Illingworth, G.D., Kelson, D.D., van Dokkum, P.G., Tran, K., 1997, astro-ph/9704090
- Kron, R. G., 1995, in *The Deep Universe*, ed. Sandage, A. R., Kron, R. G. and Longair, M. S., (Berlin: Springer-Verlag)
- McGaugh, 1996, MNRAS, 280, 337
- Nicolet, B., 1978, A&AS, 34, 1
- O’Connell, R. W. & Marcum, P., 1996, “The Ultraviolet Morphology of Galaxies” in *HST and the High Redshift Universe (37th Herstmonceux Conference)*, eds. N.R. Tanvir, A. Aragon-Salamanca, J.V. Wall, 1996.
- O’Connell, R. W., Gallagher, J. S., Hunter, D. A. & Colley, W. N., 1995, ApJ, 446: L1
- Odewahn, S. C., Windhorst, R. A., Driver, Simon P. & Keel, W. C., 1996, ApJ, 472, L13
- Ostriker, J.P., & Turner, E.L., 1979, ApJ, 234, 785
- Patterson, R.J., & Thuan, T.X., 1996, ApJS, 107, 103
- Peebles, P.J.E., 1993, *Principles of Physical Cosmology*, Princeton University, Princeton

- Guzmán, R., Gallego, J., Koo, D. C., Phillips, A. C., Lowenthal J. D., Faber, S. M., Illingworth, G. D., & Vogt, N. P., astro-ph/9704001
- Space Telescope Science Institute, 1995, “Filter Selection for the Hubble Deep Field” (Baltimore: STScI)
- Steidel, C., Giavalisco, M., Dickinson, M., & Adelberger, K. 1996, AJ, in press
- Williams, R.E., Blacker, B.S., Dickinson, M., Ferguson, H.C., Fruchter, A.S., Giavalisco, M., Gilliland, R.L., Lucas, R.A., McElroy, D.B., Petro, L.D., & Postman, M., “The Hubble Deep Field Observations,” 1995, in Science with the Hubble Space Telescope—II, P. Benvenuti, F. D. Macchetto, & E. J. Schreier, eds. (Baltimore: STScI)
- Williams, R.E. et al. 1996, AJ, 112, 1335
- Worthey, G. 1994, ApJS, 95, 107

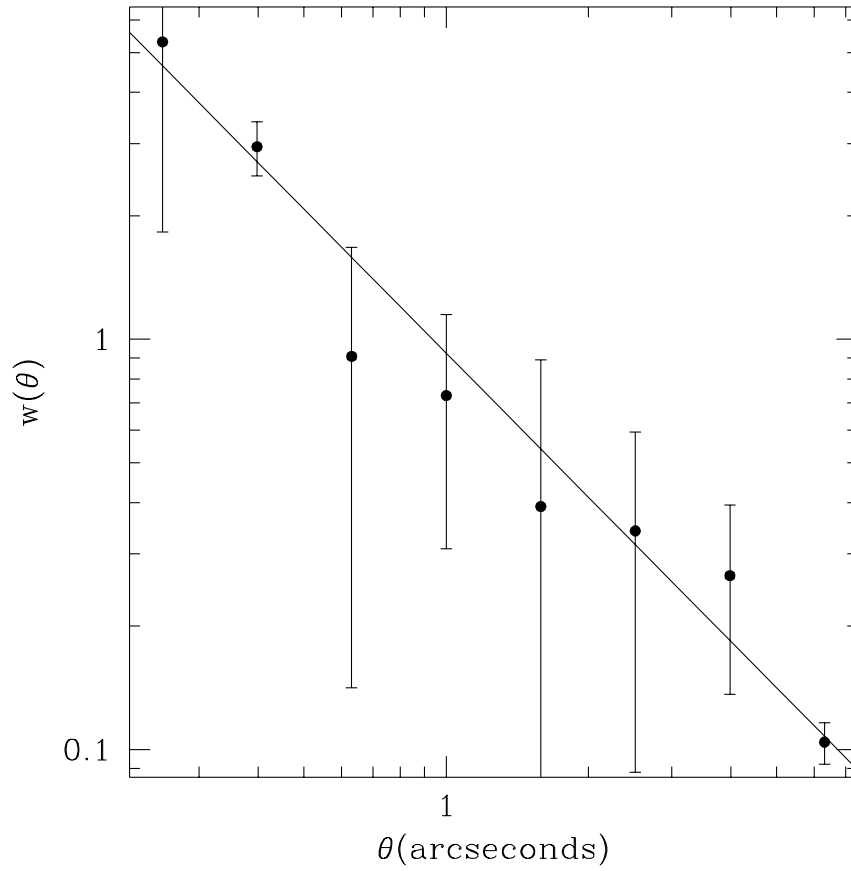


Fig. 1.— The angular correlation function of high color-redshift objects in the Hubble Deep Field. Overplotted is the best-fit power-law to the correlation,  $w_{fit} = (\theta/\theta_\ell)^\alpha$ , where  $\alpha = -1.1 \pm 0.1$  and  $\theta_\ell = 0.''89 \times 10^{\pm 0.03}$

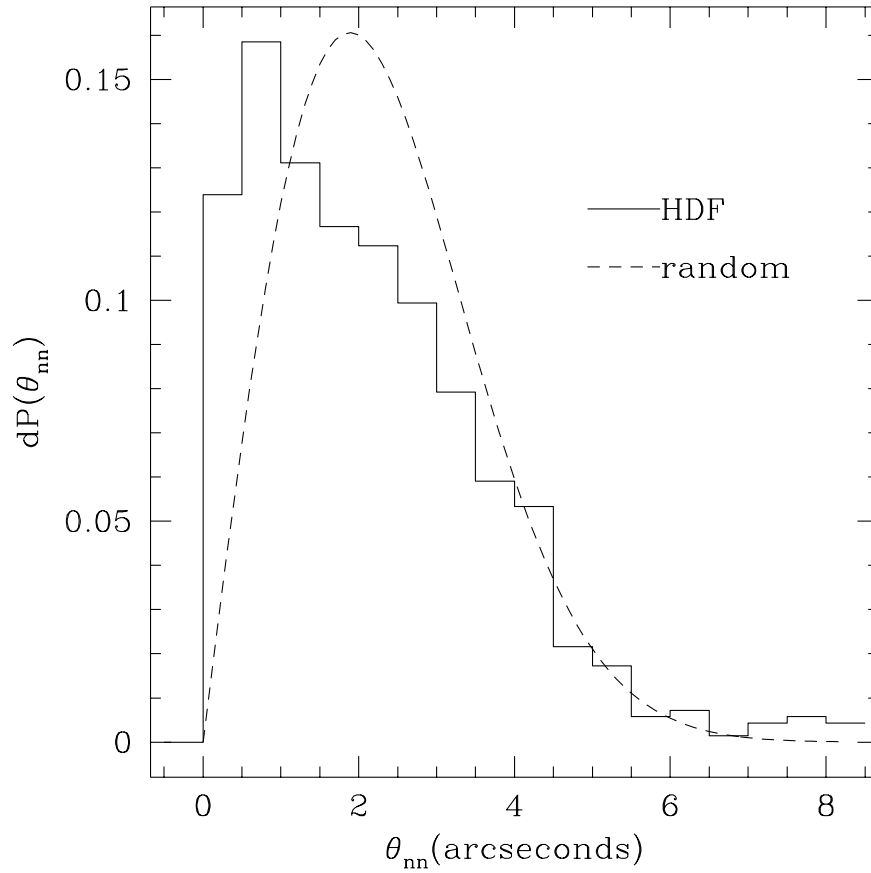


Fig. 2.— a) Distribution of nearest neighbors among high color-redshift catalog objects in the Hubble Deep Field (solid) and for a random distribution with the same number of particles (dashed). Where  $\theta_{nn}$  is the angular separation of an object and its nearest neighbor, we have plotted both the differential distribution,  $P(\theta_{nn})$ .

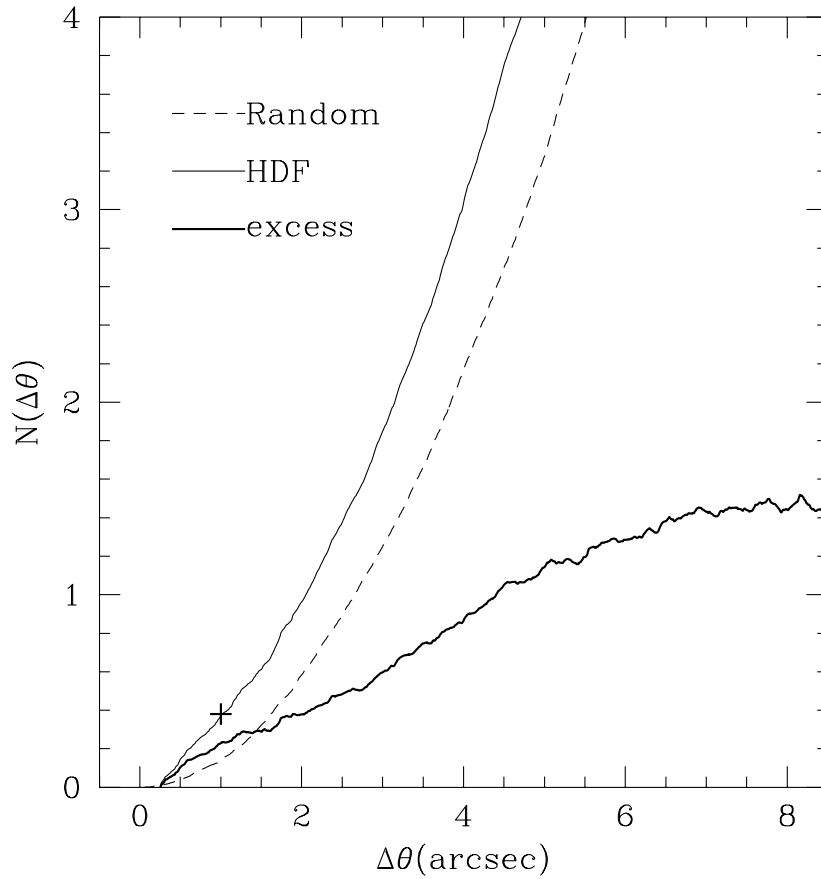


Fig. 2.— b) Cumulative distribution of all neighbors of high color-redshift objects in the Hubble Deep Field (light solid curve), the same for a random distribution (dashed curve), and the excess in the HDF (heavy solid line). The large plus sign denotes the expected number derived from the correlation function.

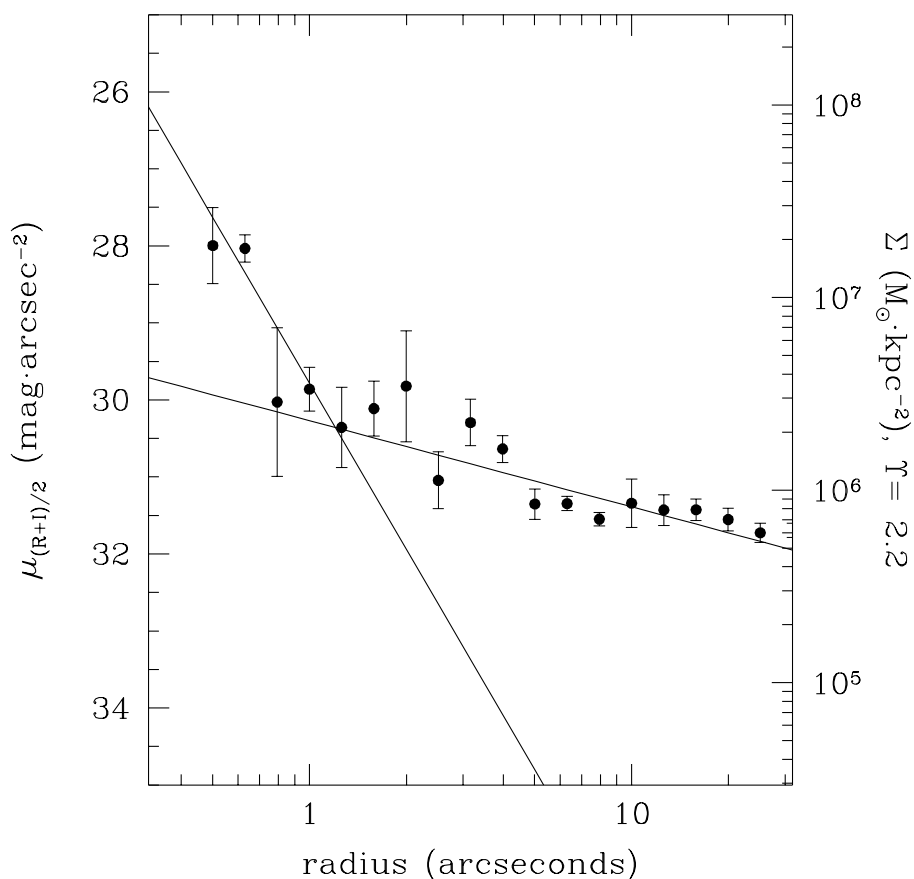


Fig. 3.— The magnitude and mass (assuming mass-to-light,  $\Upsilon = 2.2$  and distance modulus = 43.9 for  $z \sim 1$ ) in catalog objects as a function of logarithmic radius. Surface magnitude is that measured in individual catalog sources. Overplotted are two power-law fits (slope =  $-2.9 \pm 0.6$  inside one arcsecond; slope =  $-0.5 \pm 0.2$  outside one arcsecond), from which the three-dimensional mass density in the luminous sources is derived (see Text).